

Load distribution in the threaded joint subjected to bending

A. Krenevičius*, Ž. Juchnevičius**

*Vilnius Gediminas Technical University, Saulėtekio al. 11, 10223 Vilnius, Lithuania, E-mail: kron@fm.vgtu.lt

**Vilnius Gediminas Technical University, Saulėtekio al. 11, 10223 Vilnius, Lithuania, E-mail: ma@fm.vgtu.lt

1. Introduction

High stress concentrations existing at thread roots often cause fatigue failure of the connectors. Load distribution along the threads has a direct influence on the stress at thread roots. Previous analysis of load distribution in threads was mainly limited to the axial deformation of studs or bolts and has been reviewed in [1].

In practice, the loading is usually asymmetric or eccentric and this causes bending moments to be applied to constructions, rods and to the threaded joints also [2-4]. The experimental study of the effect of bending on the distribution of stress along the helix of the thread root by using photoelastic models is presented in [5].

The analytical analysis of load distribution on turns in the threaded joint subjected to bending without estimation of turns deflections is given in [6]. However to construct an analytical model for this case it is necessary to find relation between deflections of the turns and deviations of the cross-sections of stud/bolt and nut caused by bending of the threaded joint. In this paper the corresponding equation for compatibility of the displacements of the elements of threaded joint and analytical solution of this equation are presented.

2. The loads in threaded joint caused by bending

The external load of the threaded joint can be divided into two main components. It is axial load of tightening F_t and external bending moment M_f (Fig. 1).

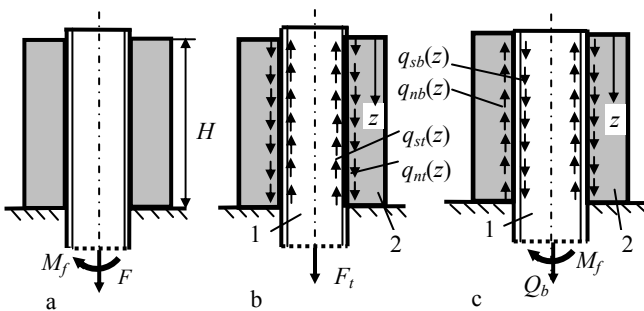


Fig. 1 Loads in threaded joint at bending: a – external loads, b – loads caused by tightening, c – loads caused by bending; 1 - stud, 2 - nut

The turns of stud are under the action of a distributed longitudinal load - force per unit length

$$q_s(z) = q_{st}(z) \pm q_{sb}(z), \quad q_{st}(z) > |q_{sb}(z)| \quad (1)$$

where $q_{st}(z)$ and $q_{sb}(z)$ are turn load intensities at coordinate z caused by tightening and bending respectively.

In opposite direction the same loads are distributed along the nut thread: $q_n(z) = q_{nt}(z) \pm q_{nb}(z)$. By using

designations we have: $|q_n(z)| = q_s(z) = q(z)$, $|q_{nt}(z)| = q_{st}(z) = q_t(z)$ and $|q_{nb}(z)| = q_{sb}(z) = q_b(z)$. Due to the longitudinal load in the thread of stud $q_b(z)$ the small axial force Q_b can arise in the stud core (Fig. 1, c).

Further the exact place of the turn load action on the helix which correspond to mean thread diameter $2R$ shall be expressed by angle α (Fig. 2).

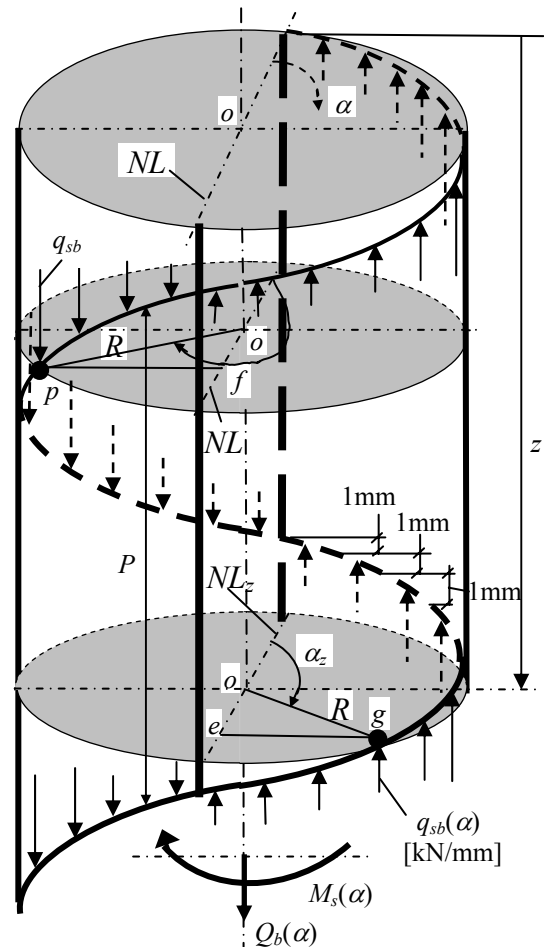


Fig. 2 Load intensity on helix turns of bended stud

This angle shows how much is turned radius R the end of which draws helix at rotating around z axis. At 2π angle of the rotation the radius R move on distance equal to the thread pitch P in direction of axis z yet. Initial location of the radius R coincides with the neutral line on initial cross-section of the stud (here $z = 0$ and $\alpha = 0$). Then relation between z and α is

$$\alpha = \frac{z}{P} 2\pi \quad (2)$$

The location of radius R in considered cross-section z (according Fig. 2 here point g and turn load

$q_{sb}(\alpha) = q_{sb}(z)$ are found) can be determined by angle α_z also. The relation between α_z and α is $\alpha_z = \alpha - 2\pi k_z$ (then $\sin \alpha_z = \sin \alpha$), where k_z is the number of full turns, which contain in length z . Really α_z is the angle between neutral line NL_z in cross-section z and radius R (Fig. 2).

Due to the action of the turn load $q_{sb}(z)$ local bending moment $m_s(\alpha)$ and the whole internal moment $M_s(\alpha)$ occur in every cross-section z of the stud also (Fig. 2)

$$m_s(\alpha) = q_{sb}(\alpha) R \sin \alpha \quad (3)$$

$$M_s(\alpha) = \int_0^\alpha m_s(\alpha) d\alpha \quad (4)$$

The corresponding opposite bending moments act in the cross-section z of the nut

$$|m_n(\alpha)| = m_s(\alpha), \quad |M_n(\alpha)| = M_s(\alpha) \quad (5)$$

The small opposite axial internal forces occur in cross-section z of the stud and nut too

$$Q_b(\alpha) = \int_0^\alpha q_b(\alpha) d\alpha \quad (6)$$

where $Q_b(z) = Q_{sb}(z) = |Q_{nb}(z)|$, $Q_{sb}(z)$ and $Q_{nb}(z)$ are axial internal forces in cross-section z of the stud and nut respectively. In cross-section $z = H$ (Fig. 1) of the stud the force $Q_{sb}(H)$ slightly changes the amount of tightening force F_t .

3. Equation for compatibility of displacements of threaded joint elements due to bending

In Fig. 3, b and Fig. 3, d displacements of cross-sections of the stud and nut and deflections of the turn pairs at turn's contact points p and g are shown. (Location of this points is shown in Fig. 2 also). For convenience of representation the cross-sections with points p and g are superposed in Fig. 3. It would be really in the circular turns case. Before deformation contact points p and g of the turns and corresponding cross-sections of the stud and nut are in the plane ss (Fig. 3, a, c). Due to bending the cross-sections of the stud and nut deviate around neutral line in opposite directions - into positions s^*s^* and $s^{**}s^{**}$ respectively (Fig. 3, b, d). These deviations are designated here as φ_s and φ_n .

In the compressed side of the stud its' turn recede from the nut turn on distance $\delta_s + \delta_n$. It is the distance between points p^* or p^{**} (Fig. 3, b). In tight threaded joint the turns contact does not disappear. Really the deflection of turns pair in this side of the joint decreases only. In the opposite side of neutral line the deflection of turns pair due to the bending increases by amount $(\delta_s + \delta_n)$. It is the distance between points g^* and g^{**} (Fig. 3, c). The deflection of the turns pair - sum of the stud and nut turns deflections $\delta_b(\alpha) = \delta_s(\alpha) + \delta_n(\alpha)$ is proportional to the turn pair load, therefore it could be expressed in the same order as in the case of tension of the threaded joint [7]

$$\delta(\alpha) = \gamma q(\alpha) \quad (7)$$

where γ is pliability of the turns pair.

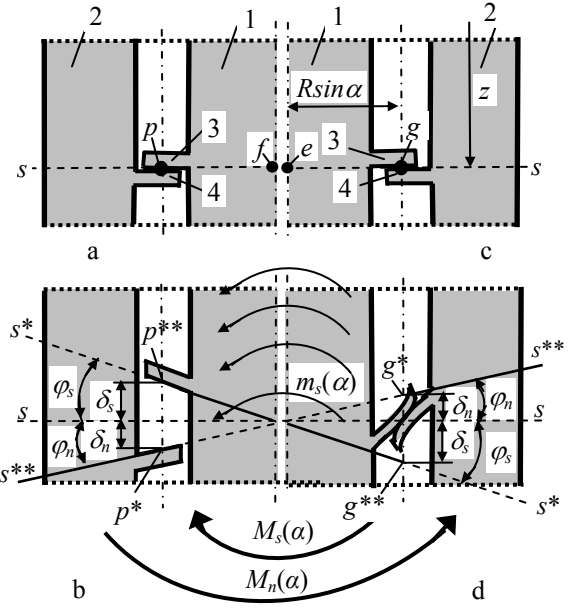


Fig. 3 Deformation of threaded joint elements due to bending: a, c – before deformation; b, d – after deformation 1 - core of the stud, 2 - wall of the nut, 3 - turns of the stud, 4 - turns of the nut

It is seen in Fig. 3 that deflection of the stud (or nut) turn has simple relation with cross-section deviation of the stud (or nut)

$$\delta_s(\alpha) = R \sin \alpha \tan \varphi_s(\alpha) \approx R \sin \alpha \varphi_s(\alpha) \quad (8)$$

$$\delta_n(\alpha) = R \sin \alpha \tan \varphi_n(\alpha) \approx R \sin \alpha \varphi_n(\alpha) \quad (9)$$

By using relation of a rod deviation to bending moment given in the theory of elasticity (and using Eqs. (3), (4), and analogous equations written for nut also) the stud and nut cross-section deviations could be expressed in the next forms

$$\begin{aligned} \varphi_s(\alpha) &= \int_0^\alpha \frac{M_s(\alpha)}{E_s I_s} d\alpha = \int_0^\alpha \frac{\int_0^\alpha m_s(\alpha) d\alpha}{E_s I_s} d\alpha = \\ &= \frac{R}{E_s I_s} \int_0^\alpha \int_0^\alpha q_{sb}(\alpha) \sin \alpha d\alpha d\alpha \end{aligned} \quad (10)$$

$$\begin{aligned} \varphi_n(\alpha) &= \int_0^\alpha \frac{M_n(\alpha)}{E_n I_n} d\alpha = \int_0^\alpha \frac{\int_0^\alpha m_n(\alpha) d\alpha}{E_n I_n} d\alpha = \\ &= \frac{R}{E_n I_n} \int_0^\alpha \int_0^\alpha q_{nb}(\alpha) \sin \alpha d\alpha d\alpha \end{aligned} \quad (11)$$

where E_s and E_n , I_s and I_n are the modulus of elasticity and the moments of inertia of the cross-sectional area for stud core and nut wall respectively.

Out of regard for Eqs. (8), (9) the compatibility of displacements of bended threaded joint elements can be expressed by the next equation

$$[\varphi_s(\alpha) + |\varphi_n(\alpha)|] R \sin \alpha = \delta(\alpha) - \delta(0) \quad (12)$$

After substituting Eqs. (7), (10), (11) into Eq. (12) and after designating $M(\alpha)=M_s(\alpha)=|M_n(\alpha)|$ and $m(\alpha)=m_s(\alpha)=|m_n(\alpha)|$ we obtain

$$R^2 \left[\frac{1}{E_s I_s} + \frac{1}{E_n I_n} \right] \int_0^\alpha \int_0^\alpha q_b(\alpha) \sin \alpha \, d\alpha \, d\alpha = \gamma \frac{q_b(\alpha)}{\sin \alpha} \quad (13)$$

By using designations

$$\frac{R^2}{\gamma} \left[\frac{1}{E_s I_s} + \frac{1}{E_n I_n} \right] = b \quad (14)$$

$$y(\alpha) = \frac{q_b(\alpha)}{\sin \alpha} \quad (15)$$

the Eq. (13) get the next expression

$$b \int_0^\alpha \int_0^\alpha y(\alpha) \sin^2 \alpha \, d\alpha \, d\alpha = y(\alpha) \quad (16)$$

After two differentiations of Eq. (16) we obtain the differential equation

$$b \int_0^\alpha y(\alpha) \sin^2 \alpha \, d\alpha = y'(\alpha) \quad (17)$$

$$by(\alpha) \sin^2 \alpha = y''(\alpha) \quad (18)$$

A boundary condition will be defined in respect to internal bending moment. First, by using Eqs. (3), (4), (15) we get

$$M(\alpha) = \int_0^\alpha m(\alpha) d\alpha = R \int_0^\alpha y(\alpha) \sin^2 \alpha \, d\alpha \quad (19)$$

Now we observe the same integral in Eq. (19) and in Eq. (17) also. Therefore

$$\frac{b}{R} M(\alpha) = y'(\alpha) \quad (20)$$

When $z=0$, $\alpha=0$ and $M(0)=0$, the Eq. (20) gives

$$y'(\alpha=0) = 0 \quad (21)$$

In the same order, when $z=H$, $\alpha_H = (H/P) 2\pi$ and $M(\alpha_H) = M_f$, from Eq. (20) we get

$$y'(\alpha_H) = \frac{b}{R} M(\alpha_H) = \frac{b}{R} M_f \quad (22)$$

4. Approximate analytical solution of the differential equation

The numerical solution of the differential equation (18) presented in the next chapter looks like exponent. (Really it is periodic – slightly wavy function). Therefore for approximate solution we provide the next expression

$$y(\alpha) = A \sinh(n\alpha) + B \cosh(n\alpha) \quad (23)$$

By using boundary conditions (21), (22) and the first derivative of Eq. (23) we obtain two factors

$$A = 0, \quad B = \frac{bM_f}{Rn \sinh(n\alpha_H)} \quad (24)$$

Further it is the need to find factor n . By equalization of Eq. (20) with the first derivative of Eq. (23) we find the internal moment

$$M(\alpha) = \frac{R}{b} y'(\alpha) = \frac{R}{b} Bn \sinh(n\alpha) \quad (25)$$

The internal moment can be found in the other way also - by substituting of Eq. (23) into Eq. (19)

$$\begin{aligned} M(\alpha) &= R \int_0^\alpha y(\alpha) \sin^2 \alpha \, d\alpha = RB \int_0^\alpha \cosh(n\alpha) \sin^2 \alpha \, d\alpha = \\ &= \frac{1}{2} RB \left[\frac{2}{n^2 + 4} (n \sin^2 \alpha - \sin 2\alpha) \cosh(n\alpha) + \right. \\ &\quad \left. + \frac{4}{(n^2 + 4)n} \sinh(n\alpha) \right] \quad (26) \end{aligned}$$

Let us to suppose that equality of expressions Eq. (25) and Eq. (26) have validity at

$$\alpha = k\pi, \quad k = 1; 2; 3; \dots \quad (27)$$

Then, by using Eq. (27) and after equalization of Eq. (25) with Eq. (26) we get

$$n^4 + 4n^2 - 2b = 0 \quad (28)$$

The solution of Eq. (28) is

$$n = \sqrt{-2 + \sqrt{4 + 2b}} \quad (29)$$

It is seen in Eq. (29) that factor n does not depend either on boundary conditions or on joint length and depend only on the deformation indices – on the factor b . In the next chapter numerically it is shown that the value of n defined by using expression (29) is right for all values of the coordinate α – not only for the cases indicated in Eq. (27).

Now, by using Eqs. (15) and (23), the following equation for the turn load intensity can be written

$$q_b(z) = \frac{bM_f}{Rn \sinh(n\alpha_H)} \cosh(n\alpha) \sin \alpha \quad (30)$$

In the stud and nut cross-sections the low internal axial forces $Q_b(z)$ act (in opposite directions) yet. The expression for these forces gives integration of the longitudinal turn load intensity due to bending

$$\begin{aligned} Q_b(\alpha) &= \int_0^\alpha q_b(\alpha) d\alpha = \int_0^\alpha y(\alpha) \sin \alpha \, d\alpha = \\ &= B \int_0^\alpha \cosh(n\alpha) \sin \alpha \, d\alpha = \\ &= \frac{B}{n^2 + 1} [n \sinh(n\alpha) \sin \alpha - \cosh(n\alpha) \cos \alpha + 1] \quad (31) \end{aligned}$$

5. Calculation results

First the differential equation (18) was solved numerically by Runge–Kutta method. It was realized by using the suite of mathematical programs Maple-9. Then the calculation for the same joint has been made by using the approximate analytical method given in the chapter 4. The object of this calculation was the threaded joint M16×2 with compressed nut (height of the nut $H = 10$ mm) – both made from grade 25X1MΦ steel.

Average indices of mechanical properties of connections grade 25X1MΦ steel: yield stress of material $R_y = 860$ MPa, tensile strength $R_m = 1010$ MPa, percentage reduction area of tension specimen $Z = 60.2\%$, module of elasticity $E = 210$ GPa. Pliability and yield load intensity for one turn pair M16×2 made from grade 25X1MΦ steel were established experimentally by the technique given in [7]: $\gamma = 3.78 \times 10^{-3}$ mm/(kN/mm) and $q_y = 14$ kN/mm.

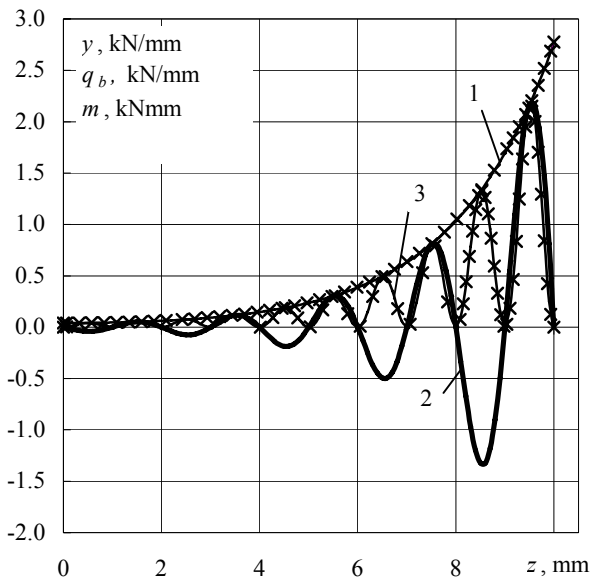


Fig. 4 Loads distribution in bent threaded joint M16: analytical solutions: 1 - $y(z)$, 2 - $q_b(z)$, 3 - $m(z)$; × - numerical solutions

The calculations of functions $y(z)$, $q_b(z)$, $m(z)$ and $M(z)$ have been performed at external bending moment $M_f = 64.5$ kNmm applied to the stud of joint (Fig. 4 and 5). In this case the ratio of nominal maximal normal stresses in stud with the yield stresses is $\sigma_{s,n,max}/R_y = 0.31$.

In Fig. 4 by solid lines are shown the variation of the functions, which have been calculated by using analytical method: $y(z)$ – by Eq. (23), $q_b(z)$ – by Eqs. (15 and 23), $m(z)$ – by Eqs. (3 and 23). The corresponding values of the above mentioned functions obtained by Runge-Kutta method in Fig. 4 are shown by criss-cross. The values of the function $y(z)$ (and values of $q_b(z)$ also) from analytical solution are miserly less than these obtained from Runge-Kutta method. For the threaded joint M16 the greatest difference is 0.8 % only.

In Fig. 5 line 1 shows the variation of the internal bending moment $M(z)$, which has been calculated by using analytical method (Eq. (26)). The values of $M(z)$ shown in Fig. 5 by criss-cross have been calculated by using Eq.(20) and derivation of the function $y(z)$ obtained from Runge-

Kutta method. In this case the greatest difference is very low also – 0.28%.

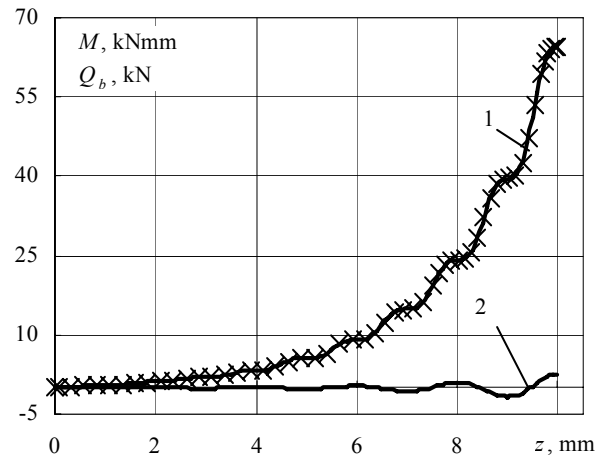


Fig. 5 Bending moment in the threaded joint M16: analytical solutions: 1 - $M(z)$, 2 - $Q_b(z)$; × - numerical solutions

Line 2 in Fig. 5 (obtained from Eq. (31)) shows periodical variation of the small axial force $Q_b(z)$ and its direction in the stud and nut caused by longitudinal turn load intensity due to the bending.

The loads distribution between turns for the real case (Fig. 1), when threaded joint (here M16×2 with $H = 0.8d = 12.8$ mm, $d = 16$ mm) is subjected to axial tightening force and to bending moment is shown in Fig. 6. In the presented example the bending is the same as above - $M_f = 64.5$ kNmm and $\sigma_{s,n,max} = 0.31R_y$. The axial (tight) nominal stresses in the stud is $\sigma_{s,n,t} = 0.5R_y$. The loads ($q_{st}(z)$) distribution in the thread due to axial tight force (curves 1 and 2 in Fig. 6) has been obtained from the method presented in [8], where the influence of runouts is estimated.

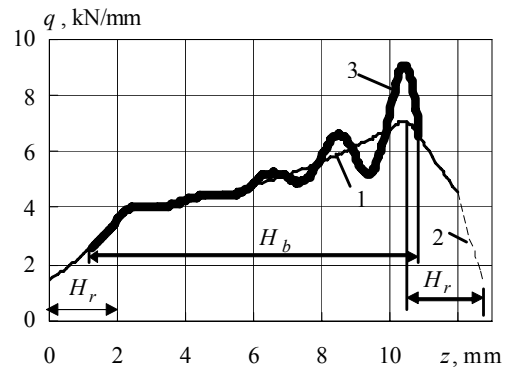


Fig. 6 Load distribution in the thread of tight stud at bending of the threaded joint M16: 1 - $q_{st}(z)$, 2 - $q_{st}(z)$ on plastically deformed part of runout, 3 - $q_s(z) = q_{st}(z) + q_{sb}(z)$

As at the worst the maximal turn load location found after tightening in the stud is in its bending plane and coincides with the location of the maximal turn load caused by bending. Then the both maximal turn loads must be summarized. For this here is assumed also that the joint is subjected to bending moment in the middle segment $H_b = 10$ mm only (Fig. 6) and practically does not acts on runouts (on segments H_r). Then the calculation results

($q_{sb}(z)$) presented in Fig. 4 can be used to determine the whole curve 3 (Fig. 6) which expresses the total load on the turns - $q_s(z) = q_{st}(z) + q_{sb}(z)$. It is necessary to notice here that direct summarizing of the maximal turn loads caused by tension and bending in the segment H_b (Fig. 6) is valid at $q_s(z) < q_y$, i.e., if deformation of the turns remains in the elastic state.

The analytical model of the load distribution in the thread caused by threaded joint bending further can be used to obtain local stresses in the roots of the stud thread for using it in a fatigue durability prediction at the engineering design.

6. Conclusions

1. The relation between deflections of the engaged turns and deviations of the stud and nut cross-sections gives the compatibility and further differential equations with respect to load distribution in the thread of the threaded joint subjected to bending.

2. The turn load intensity $q_b(z)$ and internal bending moments $M(z)$ in cross-sections of the threaded joint could be calculated by using the proposed approximate analytical solution of the differential equation. The values of $q_b(z)$ and $M(z)$ determined by analytical method and obtained by numerical (Runge-Kutta) method differ very slight – for threaded joint M16 it is 0.8% and 0.28% respectively.

References

1. **Patterson, E.** A Comparative study of methods for estimating bolt fatigue limits. -Fatigue and Fracture of Engineering Materials and Structures, 1990, v.13, No1, p.59-81.
2. **Daunys, M., Bazaras, Z., Timofeev, B.** Low cycle fatigue of materials in nuclear industry. -Mechanika. -Kaunas: Technologija, 2008, Nr.5(73), p.12-17.
3. **Leonavičius, M., Šukšta, M.** Shakedown of bolts with a one-sided propagating crack. -Journal of Civil Engineering and Management.-Vilnius: Technika, 2002, v.VIII, Nr.2, p.104-107.
4. **Atkočiūnas, J., Merkevičiūtė, A., Venskus, A., et al.** Nonlinear programming and optimal shakedown of frames. -Mechanika. -Kaunas: Technologija, 2007, Nr.2(64), p.27-33.
5. **Burguete, R., Patterson, E.** The effect of eccentric loading on the stress distribution in thread roots. -Fatigue. Fracture of Engineering Materials. Structures, 1995, v.18, No.11, p.1333-1341.
6. **Yazawa, S., and Hongo, K.** Distribution of load in screw thread of a bolt-nut connection subjected to tangential forces and bending moments. -JSME International Journal, 1988, Series I, v.31, No.2, p.174-180.
7. **Speičys, A., Krenevičius, A.** The distribution of loads on the spiral threads, taking into account plastic deformations. -Mashinovedeniye, 1987, No2, c.87-92 (in Russian).
8. **Selivonec, J., Krenevičius, A.** Distribution of load in the threads. -Mechanika. -Kaunas: Technologija, 2004, Nr.2(46), p.21-26.

A. Krenevičius, Ž. Juchnevičius

APKROVOS PASISKIRSTYMAS LENKIAMOS SRIEGINĖS JUNGTIES VIJOSE

R e z i u m ė

Sudaryta lenkiamos srieginės jungties elementų poslinkių suderinamumo lygtis. Nustatyti jos sprendiniai – skaitinis ir apytikris analitinis. Jungties M16 skaičiavimo pavyzdyje parodyta, kad abiem būdais apskaičiuotos vijų apkrovų vertės skiriasi ne daugiau kaip 0.8 procento.

A. Krenevičius, Ž. Juchnevičius

LOAD DISTRIBUTION IN THE THREADED JOINT SUBJECTED TO BENDING

S u m m a r y

This paper presents the analytical model of load distribution between turns in the threaded joint subjected to bending. The equation for the displacements compatibility of threaded joint elements is constructed. The numerical and approximate analytical solutions for this equation are obtained.

А. Крeнявичюс, Ж. Юхнявичюс

РАСПРЕДЕЛЕНИЕ НАГРУЗКИ ПО ВИТКАМ ПРИ ИЗГИБЕ РЕЗЬБОВОГО СОЕДИНЕНИЯ

Р e з ю м e

Составлено уравнение совместимости перемещений элементов изгибаемого резьбового соединения. Для этого получено дифференциальное уравнение и его решения – численное и приближенное аналитическое. В примере расчета показано, что значения нагрузок на витках соединения M16, полученные используя оба способа расчета, отличаются не более чем на 0.8 процента.

Received May 21, 2009

Accepted June 30, 2009